

RAPID GENERATION OF THE SHORTEST GENERALIZED DUBINS PATH IN FORCED LANDING

MIN TIAN^a, YINGJING SHI^{a,*}, RUI LI^a, ESTEBAN TLELO-CUAUTLE^b

^aSchool of Automation Engineering
University of Electronic Science and Technology of China
2006 Xiyuan Avenue, Chengdu, China, 611731
e-mail: shiyingjing@uestc.edu.cn

^bDepartment of Electronics
National Institute of Astrophysics, Optics and Electronics (INAOE)
Luis Enrique Erro No. 1, Puebla, Mexico 72840, Mexico

This paper investigates the problem of rapid shortest path generation during an aircraft's forced landing, where the heading angle of the target point is variable. To address the minimum turning radius constraint of the aircraft, the shortest path is determined using Dubins curves. Additionally, the shortest generalized Dubins path is selected when the heading angle of the target point is not fixed. Specifically, the paper focuses on four generalized Dubins curves which are relevant to forced landings. By comparing the lengths of these curves, the shortest curve is identified for different positional relationships between the forced landing starting and ending points, with theoretical justifications provided. Additionally, distance calculation methods for these curves are presented to determine the distance of the shortest generalized Dubins path. The effectiveness of the proposed method is confirmed through numerical simulations.

Keywords: generalized Dubins curve, path planning, forced landing.

1. Introduction

Forced landing refers to a scenario where an aircraft is compelled to land at a nearby designated landing site due to an interruption in its normal flight operations, such as the loss of engine thrust. The planning of flight paths is a critical aspect of forced landing investigations, with numerous studies dedicated to addressing this issue as documented in references (Kim *et al.*, 2020; Vána *et al.*, 2018; Izuta and Takahashi, 2017; Haghghi *et al.*, 2022; Guo *et al.*, 2021; Eng, 2011; Liu *et al.*, 2022). In the case of a fixed-wing aircraft that is restricted to forward movement and has a minimum turning radius, the flight paths must adhere to curvature constraints. Dubins (1957) introduced a technique for determining the shortest curvature-constrained path between two points with a fixed heading angle, making the Dubins path the predominant method for path planning in fixed-wing aircraft operations.

Research conducted by Dubins (1957) demonstrates that the shortest path between two points, while maintaining a specified heading angle, consists of a combination of arcs and straight line segments. These components are designated as arcs (C) and straight line segments (S), resulting in two possible configurations for the shortest path: CSC or CCC. Moreover, when considering right-turning arcs (R) and left-turning arcs (L), the shortest path can be classified into six distinct combinations: RSL, RSR, LSR, LSL, RLR, and LRL. This shortest path, comprising the aforementioned combinations, is commonly known as the shortest Dubins path.

Following the above conclusion, there has been extensive research conducted on determining the shortest Dubins paths in various scenarios. One notable scenario of study is the Dubins traveling salesman problem (DTSP), which is concerned with identifying the shortest path for visiting multiple locations. Numerous investigations have delved into this scenario (Parlangeli,

*Corresponding author

2019a; Váňa and Faigl, 2022; Chen and Shima, 2019a; Parlange, 2019b; Chen and Shima, 2019b; Drchal *et al.*, 2020; Manyam and Rathinam, 2018). Additionally, a significant body of research has been dedicated to analyzing the shortest path between an initial position with a specified heading angle and a target circle (Chen, 2020; Manyam *et al.*, 2019b; Gupta Manyam *et al.*, 2022; Manyam *et al.*, 2019a).

The papers mentioned above examined the issue in scenarios where the position and heading angle of the target point were either fixed or unfixed. This study focuses on analyzing the shortest Dubins path in another significant scenario, where the target point's position is fixed but the heading angle is variable. The rationale behind this study is that for forced landings of fixed-wing aircraft, the heading angle of the target point does not necessarily have to be fixed. Typically, the landing site for fixed-wing aircraft during forced landing is a suitable location near the aircraft, such as a lake or sandy area, making the heading angle of the aircraft insignificant when approaching the forced landing site. In this specific scenario, it is validated that the shortest Dubins path comprises only two segments, either CS type or CC type. Additionally, the shortest path is one of four potential combinations: RS, LS, RL, and LR. These Dubins curves are known as generalized Dubins curves in this scenario.

Several papers (Gao *et al.*, 2013; Ismail *et al.*, 2018) have investigated the shortest generalized Dubins path from a fixed heading angle starting point to an unfixed heading angle ending point. To be specific, Gao *et al.* (2013) proposed a solution method using the theory of Dubins curves and an analytical approach to the shortest generalized Dubins path problem. However, it is not applicable when the distance between the two points is short. Ismail *et al.* (2018) examined the shortest generalized Dubins path for any distance between the starting and ending points. However, the approach in Ismail *et al.* (2018) only considers paths involving RS and LS curves, neglecting RL and LR combinations, which may not always represent the actual shortest path between the two points.

No research has been reported yet on a direct method for determining the shortest curve among the four curves RS, LS, RL, and LR, given arbitrary positional relationships between their starting and ending points. Current engineering practices involve calculating the lengths of these curves and comparing them to identify the shortest one, which entails a complex algorithm and significant computational time. In scenarios such as forced landing, where the ending point's position is fixed but the heading angle is variable, the shortest generalized Dubins path is typically chosen as the optimal path. In the event of an emergency forced landing, it is imperative to quickly determine an optimal path for the aircraft. Furthermore, real-time calculations of the optimal path

distance between the current aircraft position and the designated forced landing site are essential to ensure the safety and success of the landing procedure. Therefore, there is a necessity to seek a fast method to generate the shortest generalized Dubins path in real-time.

Taking inspiration from the above considerations, this paper introduces a viable approach for quickly generating the shortest generalized Dubins path connecting the starting point with a fixed heading angle and the ending point with an unfixed heading angle, while accommodating any arbitrary positional configuration between these two points. Specifically, the research in this paper involves the comparison and validation of the length disparities among the four generalized Dubins curves, culminating in the determination of the shortest generalized Dubins path. Additionally, the paper outlines the methodology for calculating the shortest generalized Dubins path under the conditions of a known starting point position and heading angle, as well as the ending point position.

The main contributions of this work are twofold.

- (i) A method is proposed for quickly generating the shortest generalized Dubins path in forced landing. With this method, the optimal path is derived directly without computation and comparison of the lengths of four curves, which ensures a fast engineering solution.
- (ii) The methodology for calculating the length of shortest generalized Dubins curve is provided, with which the distance of the optimal path is analytically obtained in forced landing.

The subsequent sections of this paper are organized as follows. Section 2 presents a formal statement of the shortest generalized Dubins path problem being examined. Section 3 establishes and proves the length relationship among four generalized Dubins curves and determines the shortest generalized Dubins path. Section 4 outlines the distance calculation techniques for the four generalized Dubins curves and presents numerical simulation results to verify the correctness of the proposed methods. Finally, Section 5 demonstrates the main conclusions of this paper.

2. Preliminaries and problem statement

In the context of forced landing scenarios, the mathematical formulation of the shortest path problem can be conceptualized as follows. Consider a starting point with a specified direction and an ending point without a designated direction in the two-dimensional plane, and these points are linked through a generalized Dubins curve. The objective of this paper is to determine the shortest generalized Dubins curve connecting the two points.

Assume that vectors \mathbf{p} and \mathbf{q} are situated within the two-dimensional plane, and θ represents the angular measurement of the starting direction. The concept of “type” refers to a form of generalized Dubins curve, which is taken from RS, LS, RL, or LR. L_{type} represents the distance operation utilized for determining the generalized Dubins curve of a specific type between \mathbf{p} and \mathbf{q} . $L(\mathbf{p}, \theta, \mathbf{q})$ denotes the shortest generalized Dubins curve distance from \mathbf{p} to \mathbf{q} .

The solution of $L(\mathbf{p}, \theta, \mathbf{q})$ is dependent on the spatial relationship between \mathbf{p} and \mathbf{q} . Let \mathbf{c}_{rs} and \mathbf{c}_{ls} denote the centers of the right-turning and left-turning circles respectively, both originating from the starting point \mathbf{p} , and ρ represents the radius of these circles. When $\|\mathbf{q} - \mathbf{c}_{rs}\| < \rho$, the curves RS and RL connecting \mathbf{p} and \mathbf{q} do not exist. Similarly, when $\|\mathbf{q} - \mathbf{c}_{ls}\| < \rho$, the curves LS and LR do not exist. A common solution applied in the current references for $L(\mathbf{p}, \theta, \mathbf{q})$ can be concluded as

$$L(\mathbf{p}, \theta, \mathbf{q}) = \begin{cases} \min \{L_{RS}, L_{LS}, L_{RL}, L_{LR}\}, & \text{Case 1,} \\ \min \{L_{LS}, L_{LR}\}, & \text{Case 2,} \\ \min \{L_{RS}, L_{RL}\}, & \text{Case 3,} \end{cases} \quad (1)$$

where Case 1 is $\|\mathbf{q} - \mathbf{c}_{rs}\| \geq \rho \cap \|\mathbf{q} - \mathbf{c}_{ls}\| \geq \rho$, Case 2 is $\|\mathbf{q} - \mathbf{c}_{rs}\| < \rho$, Case 3 is $\|\mathbf{q} - \mathbf{c}_{ls}\| < \rho$.

The aim of this paper is to find out an exact solution for (1), and provide distance calculation methodologies for four generalized Dubins curves, specifically focusing on solving L_{type} .

For the sake of clarity, it is necessary to introduce some definitions:

Definition 1. For $\mathbf{s}, \mathbf{c} \in \mathbb{R}^2$, $\rho \in \mathbb{R}^+$, define $S(\mathbf{c}, \rho) = \{\mathbf{s} \mid \|\mathbf{s} - \mathbf{c}\| < \rho\}$.

Definition 2. For $\mathbf{p}, \mathbf{r}, \mathbf{x} \in \mathbb{R}^2$, $\lambda \in \mathbb{R}$, let \mathbf{r} be the direction vector of \mathbf{p} . Define line $(\mathbf{p}, \mathbf{r}) = \{\mathbf{x} \mid \mathbf{x} = \mathbf{p} + \lambda \mathbf{r}\}$.

Definition 3. For $\mathbf{r} \in \mathbb{R}^2$, let \mathbf{r} be a direction vector, and $\mathbf{r} = (x, y)^\top$. Define $\chi(\mathbf{r}) = \text{atan2}(y, x)$, $\chi(\mathbf{r}) \in [-\pi, \pi]$. Here,

$$\text{atan2}(y, x) = \begin{cases} \arctan\left(\frac{y}{x}\right), & x > 0 \\ \arctan\left(\frac{y}{x}\right) + \pi, & y \geq 0, x < 0 \\ \arctan\left(\frac{y}{x}\right) - \pi, & y < 0, x < 0 \\ \frac{\pi}{2}, & y > 0, x = 0 \\ -\frac{\pi}{2}, & y < 0, x = 0 \\ \text{undefined.} & x = y = 0 \end{cases}$$

Definition 4. For $\mathbf{a}, \mathbf{b} \in \mathbb{R}^2$, let \mathbf{a} and \mathbf{b} be direction vectors. Define $\theta_R(\mathbf{a}, \mathbf{b}) = \text{mod}(\chi(\mathbf{b}) - \chi(\mathbf{a}), 2\pi)$, $\theta_L(\mathbf{a}, \mathbf{b}) = \text{mod}(\chi(\mathbf{a}) - \chi(\mathbf{b}), 2\pi)$.

3. The shortest generalized Dubins path

In this section, we present the methodologies for determining the shortest generalized Dubins curve based

on various positional configurations between the forced landing starting and ending points. We first establish the main results of this paper. The solution of (1) can be specified as

$$L(\mathbf{p}, \theta, \mathbf{q}) = \begin{cases} L_{LR}, & \text{Case 1,} \\ L_{RL}, & \text{Case 2,} \\ L_{RS}, & \text{Case 3,} \\ L_{LS}, & \text{Case 4,} \end{cases} \quad (2)$$

where Case 1 is $\|\mathbf{q} - \mathbf{c}_{rs}\| < \rho$, Case 2 is $\|\mathbf{q} - \mathbf{c}_{ls}\| < \rho$, Case 3 is $\|\mathbf{q} - \mathbf{c}_{rs}\| \geq \rho \cap \|\mathbf{q} - \mathbf{c}_{rs}\| \leq \|\mathbf{q} - \mathbf{c}_{ls}\|$, Case 4 is $\|\mathbf{q} - \mathbf{c}_{ls}\| \geq \rho \cap \|\mathbf{q} - \mathbf{c}_{ls}\| < \|\mathbf{q} - \mathbf{c}_{rs}\|$.

In order to draw the conclusion in (2), we only need to prove that

$$\begin{cases} L_{LR} < L_{LS}, & \text{Case 1,} \\ L_{RL} < L_{RS}, & \text{Case 2,} \\ \min \{L_{RS}, L_{LS}, L_{RL}, L_{LR}\} = L_{RS}, & \text{Case 3,} \\ \min \{L_{RS}, L_{LS}, L_{RL}, L_{LR}\} = L_{LS}. & \text{Case 4.} \end{cases}$$

In the following, we provide theoretical proofs for the correctness of these methodologies.

3.1. The ending point outside the turning circles of the starting point. In this subsection, for $\|\mathbf{q} - \mathbf{c}_{rs}\| \geq \rho \cap \|\mathbf{q} - \mathbf{c}_{ls}\| \geq \rho$, we prove that

$$L(\mathbf{p}, \theta, \mathbf{q}) = \begin{cases} L_{RS}, & \|\mathbf{q} - \mathbf{c}_{rs}\| \leq \|\mathbf{q} - \mathbf{c}_{ls}\|, \\ L_{LS}, & \|\mathbf{q} - \mathbf{c}_{ls}\| < \|\mathbf{q} - \mathbf{c}_{rs}\|, \end{cases}$$

which implies that with the common tangent of circle \mathbf{c}_{rs} and circle \mathbf{c}_{ls} as the boundary, the shortest generalized Dubins curve distance is L_{RS} when \mathbf{q} is on the common tangent or on the side of \mathbf{c}_{rs} , and the shortest distance is L_{LS} when \mathbf{q} is on the side of \mathbf{c}_{ls} .

Assume that \mathbf{r}_p is the direction of \mathbf{p} , $\mathbf{i} = [1, 0]^\top$, the rotation matrix is

$$\mathbf{R}(\varphi) = \begin{bmatrix} \cos \varphi & -\sin \varphi \\ \sin \varphi & \cos \varphi \end{bmatrix},$$

so we have $\mathbf{r}_p = \mathbf{R}(\theta) \cdot \mathbf{i}$.

With the help of the above definitions, we get

$$\mathbf{c}_{rs} = \mathbf{p} + \rho \cdot \mathbf{R}\left(\chi(\mathbf{r}_p) + \frac{\pi}{2}\right) \cdot \mathbf{i}, \quad (3)$$

$$\mathbf{c}_{ls} = \mathbf{p} + \rho \cdot \mathbf{R}\left(\chi(\mathbf{r}_p) - \frac{\pi}{2}\right) \cdot \mathbf{i}. \quad (4)$$

Next, we present the methodologies for determining the shortest generalized Dubins curve in cases where \mathbf{q} is situated either on or outside the turning circles of \mathbf{p} by Lemma 1 and Theorem 1.

Lemma 1. Suppose $\mathbf{q} \notin S(\mathbf{c}_{rs}, \rho) \cup S(\mathbf{c}_{ls}, \rho)$. Then

$$\begin{cases} L_{RS} < L_{LS}, & \|\mathbf{q} - \mathbf{c}_{rs}\| < \|\mathbf{q} - \mathbf{c}_{ls}\|, \\ L_{RS} = L_{LS}, & \|\mathbf{q} - \mathbf{c}_{rs}\| = \|\mathbf{q} - \mathbf{c}_{ls}\|, \\ L_{RS} > L_{LS}. & \|\mathbf{q} - \mathbf{c}_{rs}\| > \|\mathbf{q} - \mathbf{c}_{ls}\|. \end{cases}$$

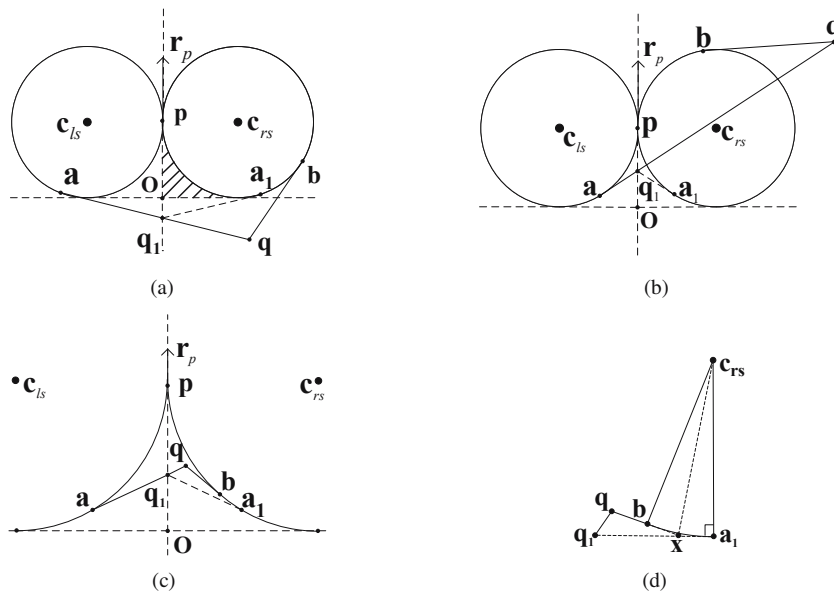


Fig. 1. The ending point is outside the two turning circles of the starting point and closer to the right-turning circle.

Proof. The lemma regards three distinct cases

- (i) It is required to prove that $L_{RS} < L_{LS}$ when $\|\mathbf{q} - \mathbf{c}_{rs}\| < \|\mathbf{q} - \mathbf{c}_{ls}\|$.
- (ii) It is required to prove that $L_{RS} = L_{LS}$ when $\|\mathbf{q} - \mathbf{c}_{rs}\| = \|\mathbf{q} - \mathbf{c}_{ls}\|$.
- (iii) It is required to prove that $L_{RS} > L_{LS}$ when $\|\mathbf{q} - \mathbf{c}_{rs}\| > \|\mathbf{q} - \mathbf{c}_{ls}\|$.

Case (i) is shown in Fig. 1. For curves L_{LS} and L_{RS} , it is clear that line $(\mathbf{q}, \mathbf{a} - \mathbf{q})$ is tangent to the circle \mathbf{c}_{ls} at \mathbf{a} , line $(\mathbf{q}, \mathbf{b} - \mathbf{q})$ is tangent to the circle \mathbf{c}_{rs} at \mathbf{b} , $\mathbf{q}_1 = \text{line}(\mathbf{q}, \mathbf{a} - \mathbf{q}) \cap \text{line}(\mathbf{p}, \mathbf{r}_p)$, and line $(\mathbf{q}_1, \mathbf{a}_1 - \mathbf{q}_1)$ is tangent to the circle \mathbf{c}_{rs} at \mathbf{a}_1 . Then

$$L_{RS} = \rho\theta_R(\mathbf{p} - \mathbf{c}_{rs}, \mathbf{b} - \mathbf{c}_{rs}) + \|\mathbf{q} - \mathbf{b}\|.$$

Based on the principle of symmetry, it can be inferred that

$$\begin{aligned} L_{LS} &= \rho\theta_L(\mathbf{p} - \mathbf{c}_{ls}, \mathbf{a} - \mathbf{c}_{ls}) + \|\mathbf{q} - \mathbf{a}\| \\ &= \rho\theta_R(\mathbf{p} - \mathbf{c}_{rs}, \mathbf{a}_1 - \mathbf{c}_{rs}) + \|\mathbf{q}_1 - \mathbf{a}_1\| \\ &\quad + \|\mathbf{q} - \mathbf{q}_1\|. \end{aligned}$$

In Fig. 1, \mathbf{o} is defined as

$$\mathbf{o} = \mathbf{p} + \rho \cdot \mathbf{R}(\chi(\mathbf{r}_p) + \pi) \cdot \mathbf{i}.$$

The shadowed region in Fig. 1 is

$$D = \left\{ \mathbf{q} \in \mathbb{R}^2 \mid \|\mathbf{q} - \mathbf{c}_{rs}\| < \|\mathbf{q} - \mathbf{c}_{ls}\|, \|\mathbf{q} - \mathbf{c}_{rs}\| \geq \rho, \|\mathbf{q} - \mathbf{o}\| < \rho, (\mathbf{p} - \mathbf{o})(\mathbf{q} - \mathbf{o}) > 0 \right\}.$$

For $\mathbf{q} \notin D$, as illustrated in Figs. 1(a) and 1(b), we have that

$$\begin{aligned} \Delta L &= L_{LS} - L_{RS} \\ &= \rho\theta_R(\mathbf{b} - \mathbf{c}_{rs}, \mathbf{a}_1 - \mathbf{c}_{rs}) \\ &\quad + \|\mathbf{q}_1 - \mathbf{a}_1\| + \|\mathbf{q} - \mathbf{q}_1\| - \|\mathbf{q} - \mathbf{b}\| > 0, \end{aligned}$$

which indicates that

$$L_{LS} > L_{RS}.$$

For $\mathbf{q} \in D$, as illustrated in Fig. 1(c), we have that

$$\begin{aligned} \Delta L &= L_{LS} - L_{RS} \\ &= \|\mathbf{q}_1 - \mathbf{a}_1\| + \|\mathbf{q} - \mathbf{q}_1\| \\ &\quad - (\rho\theta_R(\mathbf{a}_1 - \mathbf{c}_{rs}, \mathbf{b} - \mathbf{c}_{rs}) + \|\mathbf{q} - \mathbf{b}\|). \end{aligned}$$

In Fig. 1(d), \mathbf{x} is defined as

$$\mathbf{x} = \text{line}(\mathbf{q}, \mathbf{b} - \mathbf{q}) \cap \text{line}(\mathbf{a}_1, \mathbf{q}_1 - \mathbf{a}_1).$$

Then

$$\|\mathbf{q}_1 - \mathbf{x}\| + \|\mathbf{q} - \mathbf{q}_1\| > \|\mathbf{q} - \mathbf{b}\| + \|\mathbf{b} - \mathbf{x}\|. \quad (5)$$

It is a well-established fact that

$$\theta_R(\mathbf{x} - \mathbf{c}_{rs}, \mathbf{a}_1 - \mathbf{c}_{rs}) \in (0, \pi/2)$$

and

$$\theta_R(\mathbf{x} - \mathbf{c}_{rs}, \mathbf{b} - \mathbf{c}_{rs}) \in (0, \pi/2).$$

Therefore,

$$\tan \theta_R(\mathbf{a}_1 - \mathbf{c}_{rs}, \mathbf{x} - \mathbf{c}_{rs}) > \theta_R(\mathbf{a}_1 - \mathbf{c}_{rs}, \mathbf{x} - \mathbf{c}_{rs})$$

and

$$\tan \theta_R(\mathbf{x} - \mathbf{c}_{rs}, \mathbf{b} - \mathbf{c}_{rs}) > \theta_R(\mathbf{x} - \mathbf{c}_{rs}, \mathbf{b} - \mathbf{c}_{rs}),$$

so we conclude that

$$\|\mathbf{x} - \mathbf{a}_1\| + \|\mathbf{b} - \mathbf{x}\| > \rho \theta_R(\mathbf{a}_1 - \mathbf{c}_{rs}, \mathbf{b} - \mathbf{c}_{rs}). \quad (6)$$

By utilizing (5) and (6), we get

$$\begin{aligned} \|\mathbf{q}_1 - \mathbf{a}_1\| + \|\mathbf{q} - \mathbf{q}_1\| &> \rho \theta_R(\mathbf{a}_1 - \mathbf{c}_{rs}, \mathbf{b} - \mathbf{c}_{rs}) \\ &+ \|\mathbf{q} - \mathbf{b}\|. \end{aligned}$$

Hence

$$L_{LS} > L_{RS}.$$

Therefore, we prove $L_{RS} < L_{LS}$ when $\|\mathbf{q} - \mathbf{c}_{rs}\| < \|\mathbf{q} - \mathbf{c}_{ls}\|$.

For (ii), from the symmetry relationship, we have that $L_{RS} = L_{LS}$ when $\|\mathbf{q} - \mathbf{c}_{rs}\| = \|\mathbf{q} - \mathbf{c}_{ls}\|$.

For (iii), similarly to the first case, we prove that $L_{RS} > L_{LS}$ when $\|\mathbf{q} - \mathbf{c}_{rs}\| > \|\mathbf{q} - \mathbf{c}_{ls}\|$.

Thus, the demonstration of this lemma has been concluded. ■

Theorem 1. Suppose $\mathbf{q} \notin S(\mathbf{c}_{rs}, \rho) \cup S(\mathbf{c}_{ls}, \rho)$. Then

$$L(\mathbf{p}, \theta, \mathbf{q}) = \begin{cases} L_{RS}, & \|\mathbf{q} - \mathbf{c}_{rs}\| \leq \|\mathbf{q} - \mathbf{c}_{ls}\|, \\ L_{LS}, & \|\mathbf{q} - \mathbf{c}_{ls}\| < \|\mathbf{q} - \mathbf{c}_{rs}\|. \end{cases}$$

Proof. Assume that $\mathbf{q} \notin S(\mathbf{c}_{rs}, \rho) \cup S(\mathbf{c}_{ls}, \rho)$. This implies the existence of a CS curve that is shorter than the CC curve. Consequently, the shortest generalized Dubins curve between \mathbf{p} and \mathbf{q} is exclusively chosen in L_{RS} and L_{LS} . According to Lemma 1, L_{RS} is the shortest curve when $\|\mathbf{q} - \mathbf{c}_{rs}\| < \|\mathbf{q} - \mathbf{c}_{ls}\|$, L_{LS} is the shortest curve when $\|\mathbf{q} - \mathbf{c}_{rs}\| > \|\mathbf{q} - \mathbf{c}_{ls}\|$. For $\|\mathbf{q} - \mathbf{c}_{rs}\| = \|\mathbf{q} - \mathbf{c}_{ls}\|$, we have that $L_{RS} = L_{LS}$. Without loss of correctness, we specify that the order of selection and comparison of the shortest generalized Dubins curves between two points is RS, LS, RL, and LR. Consequently, L_{RS} is identified as the shortest curve when $\|\mathbf{q} - \mathbf{c}_{rs}\| = \|\mathbf{q} - \mathbf{c}_{ls}\|$.

Hence, the proof of this theorem is completed. ■

3.2. The ending point inside the turning circles of the starting point. In this subsection, for $\|\mathbf{q} - \mathbf{c}_{rs}\| < \rho$ or $\|\mathbf{q} - \mathbf{c}_{ls}\| < \rho$, we prove that

$$L(\mathbf{p}, \theta, \mathbf{q}) = \begin{cases} L_{LR}, & \|\mathbf{q} - \mathbf{c}_{rs}\| < \rho, \\ L_{RL}, & \|\mathbf{q} - \mathbf{c}_{ls}\| < \rho, \end{cases}$$

which implies that the distance of a CC-type curve is shorter than the distance of a CS-type curve when \mathbf{q} is inside the two turning circles of \mathbf{p} .

Remark 1. Suppose that $\mathbf{q} \in S(\mathbf{c}_{rs}, \rho)$. It is known that the LS curve exists and is unique. Regarding the LR curve, it is observed that there are two distinct LR-type curves

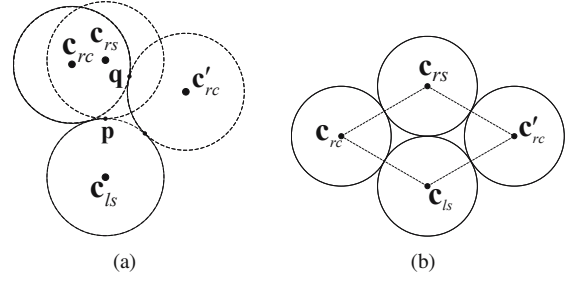


Fig. 2. The range of the starting arc radian of LR curve.

which are formed by a left-turning arc and a right-turning arc, depending on the initial arc with different radians. Since it is not possible for a point inside the circle to lead to a straight line tangent to that circle, the RS curve does not exist. Additionally, due to the imposed turning restriction, the ending point of the RL curve must lie outside the circle \mathbf{c}_{rs} , which leads to the non-existence of the RL curve as well. Therefore, to determine the shortest generalized Dubins curve, we only need to compare one LS curve and two LR curves. Similarly, we only need to compare one RS curve and two RL curves to determine the shortest generalized Dubins curve when $\mathbf{q} \in S(\mathbf{c}_{ls}, \rho)$.

Subsequently, by Lemma 2, Lemma 3, Lemma 4, Lemma 5, and Theorem 2, we obtain the methods for selecting the shortest generalized Dubins curve when \mathbf{q} is inside the turning circles of \mathbf{p} .

Lemma 2. Suppose that $\mathbf{q} \in S(\mathbf{c}_{rs}, \rho) \cup S(\mathbf{c}_{ls}, \rho)$ and θ_s represents the starting arc angle of the CC-type generalized Dubins curve connecting \mathbf{p} and \mathbf{q} . Then $\theta_s \in (0, \pi/3) \cup (5\pi/3, 2\pi)$.

Proof. The lemma regards two distinct cases

$$(i) \quad \mathbf{q} \in S(\mathbf{c}_{rs}, \rho),$$

$$(ii) \quad \mathbf{q} \in S(\mathbf{c}_{ls}, \rho).$$

For Case (i), in accordance with Remark 1, the CC-type generalized Dubins curve exclusively features the LR curve, with the RL curve being absent. There are two cases for the position of the LR curve's right-turning circle center, which is illustrated in Fig. 2(a). The centers of these circles are denoted as \mathbf{c}_{rc} and \mathbf{c}'_{rc} , with their respective positions determined by

$$\mathbf{c}_{rc} = \mathbf{c}_{ls} + 2\rho \cdot \mathbf{R}(\chi_1 - \chi_2) \cdot \mathbf{i}, \quad (7)$$

$$\mathbf{c}'_{rc} = \mathbf{c}_{ls} + 2\rho \cdot \mathbf{R}(\chi_1 + \chi_2) \cdot \mathbf{i}, \quad (8)$$

where

$$\chi_1 = \chi(\mathbf{q} - \mathbf{c}_{ls}),$$

$$\chi_2 = \arccos\left(\frac{3\rho^2 + \|\mathbf{q} - \mathbf{c}_{ls}\|^2}{4\rho\|\mathbf{q} - \mathbf{c}_{ls}\|}\right).$$

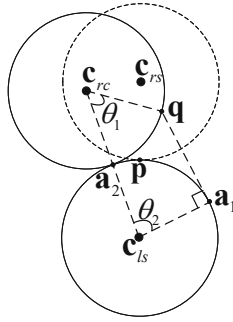


Fig. 3. The ending point is inside the the right-turning circle of the starting point.

Here, χ_2 is solved by the cosine theorem.

For c_{rc} , we have $\theta_s = \theta_L(c_{rs} - c_{ls}, c_{rc} - c_{ls}) > 0$. θ_s reaches a maximum value of $\pi/3$ when circle c_{rc} and circle c_{rs} are tangent to each other, which is illustrated in Fig. 2(b). Thus $\theta_s \in (0, \pi/3)$.

For c'_{rc} , we have $\theta_s = \theta_L(c_{rs} - c_{ls}, c'_{rc} - c_{ls}) < 2\pi$. θ_s reaches a minimum value of $5\pi/3$ when circle c'_{rc} and circle c_{rs} are tangent to each other, which is illustrated in Fig. 2(b). Thus $\theta_s \in (5\pi/3, 2\pi)$.

Therefore, we have proven that $\theta_s \in (0, \pi/3) \cup (5\pi/3, 2\pi)$ when $\mathbf{q} \in S(c_{rs}, \rho)$.

For Case (ii), by employing the aforementioned methods and steps, similarly, we prove that $\theta_s \in (0, \pi/3) \cup (5\pi/3, 2\pi)$.

Therefore, the proof of this lemma is completed. ■

Inspired by Lemma 2, we will discuss the length relations of the CC and CS-type curves for $\theta_s \in (0, \pi/3)$ and $\theta_s \in (5\pi/3, 2\pi)$, respectively, when $\mathbf{q} \in S(c_{rs}, \rho) \cup S(c_{ls}, \rho)$. We first discuss the case of $\theta_s \in (0, \pi/3)$, where the distance operations of the CC-type generalized Dubins curve is denoted as L_{RL} and L_{LR} . Then we compare L_{RL} and L_{LS} when $\mathbf{q} \in S(c_{rs}, \rho)$.

The situation is shown in Fig. 3, where line $(\mathbf{q}, \mathbf{a}_1 - \mathbf{q})$ is tangent to the circle c_{ls} at \mathbf{a}_1 and circle c_{ls} is tangent to the circle c_{rc} at \mathbf{a}_2 . Then

$$\begin{aligned} L_{LS} &= \rho\theta_L(\mathbf{p} - \mathbf{c}_{ls}, \mathbf{a}_2 - \mathbf{c}_{ls}) \\ &\quad + \rho\theta_L(\mathbf{a}_2 - \mathbf{c}_{ls}, \mathbf{a}_1 - \mathbf{c}_{ls}) + \|\mathbf{q} - \mathbf{a}_1\|, \\ L_{LR} &= \rho\theta_L(\mathbf{p} - \mathbf{c}_{ls}, \mathbf{a}_2 - \mathbf{c}_{ls}) \\ &\quad + \rho\theta_R(\mathbf{a}_2 - \mathbf{c}_{rc}, \mathbf{q} - \mathbf{c}_{rc}). \end{aligned}$$

Consequently, we have

$$\begin{aligned} \Delta L &= L_{LR} - L_{LS} \\ &= \rho\theta_R(\mathbf{a}_2 - \mathbf{c}_{rc}, \mathbf{q} - \mathbf{c}_{rc}) \\ &\quad - \rho\theta_L(\mathbf{a}_2 - \mathbf{c}_{ls}, \mathbf{a}_1 - \mathbf{c}_{ls}) - \|\mathbf{q} - \mathbf{a}_1\|. \end{aligned} \tag{9}$$

Let $\theta_1 = 2\pi - \theta_R(\mathbf{a}_2 - \mathbf{c}_{rc}, \mathbf{q} - \mathbf{c}_{rc})$, $\theta_2 = 2\pi - \theta_L(\mathbf{a}_2 - \mathbf{c}_{ls}, \mathbf{a}_1 - \mathbf{c}_{ls})$. According to the cosine theorem, we have

$$\|\mathbf{q} - \mathbf{c}_{ls}\| = \rho \cdot \sqrt{5 - 4 \cos \theta_1},$$

which yields

$$\begin{aligned} \|\mathbf{q} - \mathbf{a}_1\| &= \sqrt{\|\mathbf{q} - \mathbf{c}_{ls}\|^2 - \|\mathbf{a}_1 - \mathbf{c}_{ls}\|^2} \\ &= 2\rho \cdot \sqrt{1 - \cos \theta_1}. \end{aligned} \tag{10}$$

With (9) and (10), ΔL can be rewritten as

$$\Delta L = \rho \cdot (\theta_2 - \theta_1 - 2\sqrt{1 - \cos \theta_1}). \tag{11}$$

In reference to the LR curve depicted in Fig. 3, since the circle c_{rc} can be regarded as circle c_{rs} rotated counterclockwise around the circle c_{ls} by a specific angle, \mathbf{q} lies on the right side of the circle c_{rc} when $\mathbf{q} \in S(c_{rs}, \rho)$. Thus we have $\theta_1 \in (0, \pi)$.

Let

$$Z = \theta_2 - \theta_1 - 2\sqrt{1 - \cos \theta_1}, \tag{12}$$

where $\theta_1 \in (0, \pi)$ and $\theta_2 \in (0, \pi/2]$. It is known that comparing the size relationship between L_{LR} and L_{LS} is equivalent to comparing the size relationship between Z and 0.

From (12), we know that the sign of Z depends on θ_1 and θ_2 . For θ_1 and θ_2 , we derive some conclusions as follows.

As illustrated in Fig. 3, we have

$$\begin{aligned} \|\mathbf{q} - \mathbf{a}_2\| &= 2\rho \sin \frac{\theta_1}{2}, \\ \|\mathbf{a}_1 - \mathbf{a}_2\| &= 2\rho \sin \frac{\theta_2}{2}, \\ \theta_R(\mathbf{a}_2 - \mathbf{a}_1, \mathbf{q} - \mathbf{a}_1) &= \frac{\theta_2}{2}, \\ \theta_R(\mathbf{a}_1 - \mathbf{q}, \mathbf{a}_2 - \mathbf{q}) &= \pi - \theta_2 - \frac{\theta_1}{2}. \end{aligned}$$

From the sine theorem, it follows that

$$\frac{2\rho \sin \frac{\theta_1}{2}}{\sin \frac{\theta_2}{2}} = \frac{2\rho \sin \frac{\theta_2}{2}}{\sin(\pi - \theta_2 - \frac{\theta_1}{2})}. \tag{13}$$

Simplify (13) as

$$\cos(\theta_1 + \theta_2) - 2 \cos \theta_2 + 1 = 0. \tag{14}$$

Then we obtain

$$\begin{aligned} \theta_1 &= -\theta_2 + \arccos(-1 + 2 \cos \theta_2), \\ 0 &< \theta_1 + \theta_2 \leq \pi \end{aligned} \tag{15}$$

and

$$\begin{aligned} \theta_1 &= 2\pi - \theta_2 - \arccos(-1 + 2 \cos \theta_2) \\ \theta_1 + \theta_2 &> \pi. \end{aligned} \tag{16}$$

Next, we give a result to illustrate the size relationship between Z and 0.

Lemma 3. Suppose that $\mathbf{q} \in S(\mathbf{c}_{rs}, \rho)$. For $Z = \theta_2 - \theta_1 - 2\sqrt{1 - \cos \theta_1}$, where $\theta_1 \in (0, \pi)$ and $\theta_2 \in (0, \pi/2]$, we have $Z < 0$.

Proof. We prove that $Z < 0$ by analyzing the derivative $dZ/d\theta_2$ and examining the boundary value of Z in relation to θ_2 .

According to (12), we get

$$\frac{dZ}{d\theta_2} = 1 - \frac{d\theta_1}{d\theta_2} - \frac{\sin \theta_1}{\sqrt{1 - \cos \theta_1}} \frac{d\theta_1}{d\theta_2}, \quad (17)$$

which needs the solution for $d\theta_1/d\theta_2$.

From (15) and (16), there are two cases of the relationship between θ_1 and θ_2 . For $0 < \theta_1 + \theta_2 \leq \pi$, as illustrated in Fig. 3, $\theta_1 = \pi/2$ and $\theta_2 = \pi/2$ must hold simultaneously. Thus, it is sufficient to examine the scenario where $\theta_1 = \theta_2 = \pi/2$, and the case where $\theta_1 \neq \pi/2, \theta_2 \neq \pi/2$.

Therefore, this lemma will be proved in three cases as follows.

(i) Case of $\theta_1 = \theta_2 = \pi/2$.

From (12), we get $Z = \theta_2 - \theta_1 - 2\sqrt{1 - \cos \theta_1} = -2 < 0$.

(ii) Case of $\theta_1 + \theta_2 > \pi$.

According to (16), we determine the derivative of θ_1 with respect to θ_2 as

$$\frac{d\theta_1}{d\theta_2} = -1 - \sqrt{\frac{1}{\cos \theta_2} + 1}. \quad (18)$$

By combining (17) and (18), we deduce that

$$\frac{dZ}{d\theta_2} = 1 + \left(1 + \sqrt{1 + \cos \theta_1}\right) \left(1 + \sqrt{\frac{1}{\cos \theta_2} + 1}\right) > 0,$$

which indicates that Z increases monotonically when $\theta_2 \in (0, \pi/2)$, so we have $Z < Z_{\theta_2=\pi/2} = -2 < 0$.

(iii) Case of $\theta_1 + \theta_2 \leq \pi, \theta_1 \neq \pi/2, \theta_2 \neq \pi/2$.

From (15), we have

$$\frac{d\theta_1}{d\theta_2} = -1 + \sqrt{\frac{1}{\cos \theta_2} + 1}. \quad (19)$$

By combining (17) and (19), we obtain

$$\begin{aligned} \frac{dZ}{d\theta_2} &= 1 - \left(1 + \sqrt{1 + \cos \theta_1}\right) \\ &\quad \times \left(-1 + \sqrt{\frac{1}{\cos \theta_2} + 1}\right). \end{aligned} \quad (20)$$

Since it is difficult to directly determine the positive or negative parts of $dZ/d\theta_2$ from (20), we enlarge $dZ/d\theta_2$, where we need to compare θ_1 and θ_2 .

According to (15), define

$$\begin{aligned} f(\theta_2) &= \theta_1 - \theta_2 \\ &= -2\theta_2 + \arccos(-1 + 2\cos \theta_2), \end{aligned}$$

where $\theta_2 \in (0, \pi/2)$. Taking the derivative of $f(\theta_2)$ with respect to θ_2 , we get

$$\frac{df(\theta_2)}{d\theta_2} = -2 + \sqrt{1 + \frac{1}{\cos \theta_2}}, \quad \theta_2 \in \left(0, \frac{\pi}{2}\right).$$

It is easy to see that $df(\theta_2)/d\theta_2$ increases monotonically for $\theta_2 \in (0, \pi/2)$. Due to

$$\left. \frac{df(\theta_2)}{d\theta_2} \right|_{\theta_2=0} < 0,$$

$$\left. \frac{df(\theta_2)}{d\theta_2} \right|_{\theta_2=\frac{\pi}{2}} > 0,$$

we know that $df(\theta_2)/d\theta_2$ has only one zero point in $\theta_2 \in (0, \pi/2)$, which is $\arccos(1/3)$. Therefore, $f(\theta_2)$ decreases monotonically when $\theta_2 \in (0, \arccos(1/3)]$ and increases monotonically when $\theta_2 \in (\arccos(1/3), \pi/2)$. Since $f(0) = f(\pi/2) = 0$, we have $f(\theta_2) < 0$ when $\theta_2 \in (0, \pi/2)$, which indicates that $\theta_1 < \theta_2$.

Based on the aforementioned conclusion, from (20) we have

$$\frac{dZ}{d\theta_2} < h(\theta_2),$$

where

$$\begin{aligned} h(\theta_2) &= 1 - \left(1 + \sqrt{1 + \cos \theta_2}\right) \\ &\quad \times \left(-1 + \sqrt{\frac{1}{\cos \theta_2} + 1}\right). \end{aligned}$$

Let $t = \cos \theta_2 \in (0, 1)$. Then

$$\begin{aligned} h(\theta_2) &= g(t) \\ &= 1 - (1 + \sqrt{1+t}) \left(-1 + \sqrt{\frac{1}{t} + 1}\right). \end{aligned}$$

Taking the derivative of $g(t)$ with respect to t , we get

$$\begin{aligned} \frac{dg(t)}{dt} &= \frac{1}{2\sqrt{1+t}} + \frac{1}{2t\sqrt{t(t+1)}} \\ &\quad + \frac{1}{2t\sqrt{t}} - \frac{1}{2\sqrt{t}} > 0, \end{aligned}$$

which shows that $g(t)$ increases monotonically when $t \in (0, 1)$, so we have $g(t) < g(1) = 0$. Hence, we get

$$\frac{dZ}{d\theta_2} < h(\theta_2) = g(t) < 0,$$

which shows that Z decreases monotonically when $\theta_2 \in (0, \pi/2)$. From (12), we get

$$Z < Z_{\theta_2=0} = 0.$$

Thus, the proof of this lemma is completed. ■

Next, we give a conclusion in Lemma 4 based on the above analysis.

Lemma 4. Suppose that $\mathbf{q} \in S(\mathbf{c}_{rs}, \rho) \cup S(\mathbf{c}_{ls}, \rho)$ and $\theta_s \in (0, \pi/3)$ for the CC-type generalized Dubins curve connecting \mathbf{p} and \mathbf{q} , where the distance operation of CC-type curve is denoted as L_{RL} and L_{LR} . We have

$$\begin{cases} L_{LR} < L_{LS}, & \|\mathbf{q} - \mathbf{c}_{rs}\| < \rho, \\ L_{RL} < L_{RS}, & \|\mathbf{q} - \mathbf{c}_{ls}\| < \rho. \end{cases}$$

Proof. The lemma discusses two distinct cases

(i) It is required to prove that $L_{LR} < L_{LS}$ when $\|\mathbf{q} - \mathbf{c}_{rs}\| < \rho$.

(ii) It is required to prove that $L_{RL} < L_{RS}$ when $\|\mathbf{q} - \mathbf{c}_{ls}\| < \rho$.

For Case (i), with (9), (11), (12), and Lemma 3, we get $L_{LR} < L_{LS}$ when $\|\mathbf{q} - \mathbf{c}_{rs}\| < \rho$.

For Case (ii), similarly, we have that $L_{RL} < L_{RS}$ when $\|\mathbf{q} - \mathbf{c}_{ls}\| < \rho$.

Therefore, the proof of this lemma is completed. ■

Next, we discuss the length relations between CC and CS-type curves when $\theta_s \in (5\pi/3, 2\pi)$.

Lemma 5. Suppose that $\mathbf{q} \in S(\mathbf{c}_{rs}, \rho) \cup S(\mathbf{c}_{ls}, \rho)$ and $\theta_s \in (5\pi/3, 2\pi)$ for the CC-type generalized Dubins curve between \mathbf{p} and \mathbf{q} . Then if the distance operations of CC-type generalized Dubins curve denoted are L'_{RL} and L'_{LR} , we have the following relationships:

$$\begin{cases} L'_{LR} > L_{LS}, & \|\mathbf{q} - \mathbf{c}_{rs}\| < \rho, \\ L'_{RL} > L_{RS}, & \|\mathbf{q} - \mathbf{c}_{ls}\| < \rho. \end{cases}$$

Proof. The lemma outlines two distinct cases

(i) It is required to prove that $L'_{LR} > L_{LS}$ when $\|\mathbf{q} - \mathbf{c}_{rs}\| < \rho$.

(ii) It is required to prove that $L'_{RL} > L_{RS}$ when $\|\mathbf{q} - \mathbf{c}_{ls}\| < \rho$.

Case (i) is shown in Fig. 4, where the circle c_{ls} is tangent to the circle c'_{rc} at \mathbf{a}_3 . Then

$$L'_{LR} = \rho\theta_L(\mathbf{p} - \mathbf{c}_{ls}, \mathbf{a}_3 - \mathbf{c}_{ls}) + \rho\theta_R(\mathbf{a}_3 - \mathbf{c}'_{rc}, \mathbf{q} - \mathbf{c}'_{rc}).$$

Consequently, we have

$$\begin{aligned} \Delta L' &= L'_{LR} - L_{LS} \\ &= \rho\theta_L(\mathbf{a}_1 - \mathbf{c}_{ls}, \mathbf{a}_3 - \mathbf{c}_{ls}) \\ &\quad + \rho\theta_R(\mathbf{a}_3 - \mathbf{c}'_{rc}, \mathbf{q} - \mathbf{c}'_{rc}) - \|\mathbf{q} - \mathbf{a}_1\| > 0, \end{aligned}$$

which means $L'_{LR} > L_{LS}$.

For Case (ii), using the above methods and steps, similarly, we prove that $L'_{RL} > L_{RS}$ when $\|\mathbf{q} - \mathbf{c}_{ls}\| < \rho$.

Thus, the proof of this lemma is completed. ■

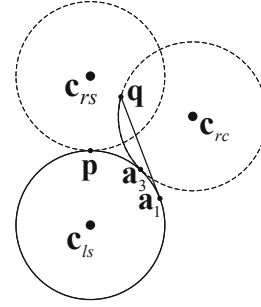


Fig. 4. The ending point is inside the right-turning circle of the starting point.

Next, we give the methods for selecting the shortest generalized Dubins curve when \mathbf{q} is inside the turning circles of \mathbf{p} .

Theorem 2. Suppose that $\mathbf{q} \in S(\mathbf{c}_{rs}, \rho) \cup S(\mathbf{c}_{ls}, \rho)$. Then

$$L(\mathbf{p}, \theta, \mathbf{q}) = \begin{cases} L_{LR}, & \|\mathbf{q} - \mathbf{c}_{rs}\| < \rho, \\ L_{RL}, & \|\mathbf{q} - \mathbf{c}_{ls}\| < \rho. \end{cases}$$

Proof. With Remark 1, Lemma 2, Lemma 4, and Lemma 5, we get $L_{LR} < L_{LS} < L'_{LR}$ when $\|\mathbf{q} - \mathbf{c}_{rs}\| < \rho$ and $L_{RL} < L_{RS} < L'_{RL}$ when $\|\mathbf{q} - \mathbf{c}_{ls}\| < \rho$. Thus, the proof is completed. ■

4. Distance calculation methods and simulations

In this section, distance calculation methods for four generalized Dubins curves are presented. By the presented distance calculation methods, the numerical simulation results are utilized to verify the correctness of the proposed method for selecting the shortest generalized Dubins curve.

4.1. Distance calculation methods of four curves. As detailed in Section 3, \mathbf{p} , \mathbf{r}_p and \mathbf{q} represent the starting point's position, starting point's direction, and ending point's position, respectively. Once \mathbf{p} , \mathbf{r}_p and \mathbf{q} are given, we determine the distance calculation methods for the four generalized Dubins curves as follows.

It is established that the determination of the center points of the turning circles plays a crucial role in the computation of the distances associated with generalized Dubins curves. The center points \mathbf{c}_{rs} , \mathbf{c}_{ls} and \mathbf{c}_{rc} are obtained from (3), (4) and (7), respectively. The center of the left-turning circle of RL curve is denoted as \mathbf{c}_{lc} , and, in a similar manner as described in (7), we have

$$\mathbf{c}_{lc} = \mathbf{c}_{rs} + 2\rho \cdot \mathbf{R}(\chi_1 + \chi_2) \cdot \mathbf{i}, \quad (21)$$

where

$$\chi_1 = \chi(\mathbf{q} - \mathbf{c}_{rs}),$$

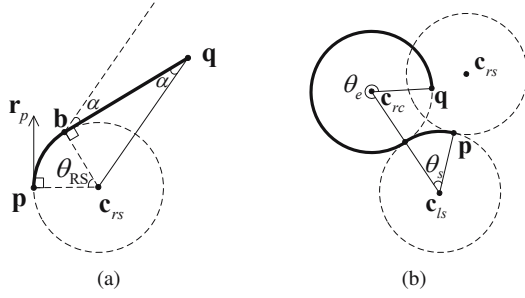


Fig. 5. The distance calculation of generalized Dubins curves: the distance calculation of an RS curve (a), the distance calculation of an LR curve (b).

$$\chi_2 = \arccos \left(\frac{3\rho^2 + \|\mathbf{q} - \mathbf{c}_{rs}\|^2}{4\rho\|\mathbf{q} - \mathbf{c}_{rs}\|} \right).$$

Here, χ_2 is solved by the cosine theorem.

As shown in Section 2, “type” refers to a form of generalized Dubins curve, which is taken from RS, LS, RL, or LR. Then we introduce θ_{type} to denote the arc radian of the generalized Dubins curve of a specific type. The computation of distance for the RS curve is illustrated in Fig. 5(a). For RS curve, line $(\mathbf{q}, \mathbf{b} - \mathbf{q})$ is tangent to the circle \mathbf{c}_{rs} at \mathbf{b} then we have

$$L_{RS} = \rho\theta_{RS} + \|\mathbf{q} - \mathbf{b}\|, \quad (22)$$

where

$$\|\mathbf{q} - \mathbf{b}\| = \sqrt{\|\mathbf{q} - \mathbf{c}_{rs}\|^2 - \rho^2}. \quad (23)$$

Subsequently, we calculate θ_{RS} , as illustrated in Fig. 5(a),

$$\theta_{RS} = \text{mod}(\chi(\mathbf{q} - \mathbf{b}) - \chi(\mathbf{r}_p), 2\pi),$$

where the function ‘mod’ ensures that θ_{RS} is positive. Make a straight line through \mathbf{b} parallel to line $(\mathbf{c}_{rs}, \mathbf{q} - \mathbf{c}_{rs})$, then the direction vector of the straight line is $\mathbf{q} - \mathbf{c}_{rs}$.

Let

$$\alpha = \arcsin \left(\frac{\rho}{\|\mathbf{q} - \mathbf{c}_{rs}\|} \right),$$

which is shown in Fig. 5(a). Therefore, we obtain

$$\chi(\mathbf{q} - \mathbf{b}) = \chi(\mathbf{q} - \mathbf{c}_{rs}) + \alpha.$$

Subsequently, we have

$$\theta_{RS} = \text{mod}(\chi', 2\pi), \quad (24)$$

where

$$\chi' = \chi(\mathbf{q} - \mathbf{c}_{rs}) + \arcsin \left(\frac{\rho}{\|\mathbf{q} - \mathbf{c}_{rs}\|} \right) - \chi(\mathbf{r}_p).$$

With (22), (23), and (24), we get the method for calculating the distance of the RS curve.

Similarly, we have the distance calculation method of the LS curve as follows. We have that

$$L_{LS} = \rho\theta_{LS} + \sqrt{\|\mathbf{q} - \mathbf{c}_{ls}\|^2 - \rho^2},$$

where

$$\theta_{LS} = \text{mod}(\chi', 2\pi),$$

$$\chi' = \chi(\mathbf{r}_p) - \chi(\mathbf{q} - \mathbf{c}_{ls}) + \arcsin \left(\frac{\rho}{\|\mathbf{q} - \mathbf{c}_{ls}\|} \right).$$

The computation of the distance for the LR curve is illustrated in Fig. 5(b), where θ_s presents the starting arc angle of the curve and θ_e presents the ending arc angle of the curve. Thus we have

$$L_{LR} = \rho\theta_{LR} = \rho(\theta_s + \theta_e). \quad (25)$$

As illustrated in Fig. 5(b), the starting arc of the LR curve involves a left turn, so that

$$\theta_s = \text{mod}(\chi(\mathbf{p} - \mathbf{c}_{ls}) - \chi(\mathbf{c}_{rc} - \mathbf{c}_{ls}), 2\pi), \quad (26)$$

where the function ‘mod’ ensures that θ_s is positive. The ending arc of the LR curve involves a right turn, so

$$\theta_e = \text{mod}(\chi(\mathbf{q} - \mathbf{c}_{rc}) - \chi(\mathbf{c}_{ls} - \mathbf{c}_{rc}), 2\pi), \quad (27)$$

where the function ‘mod’ ensures that θ_e is positive.

With (25), (26), and (27), we get the method for calculating the distance of LR curve.

Similarly, we have the distance calculation method of RL curve as follows. We have that

$$L_{RL} = \rho\theta_{RL} = \rho(\theta_s + \theta_e),$$

where

$$\theta_s = \text{mod}(\chi(\mathbf{c}_{lc} - \mathbf{c}_{rs}) - \chi(\mathbf{p} - \mathbf{c}_{rs}), 2\pi),$$

$$\theta_e = \text{mod}(\chi(\mathbf{c}_{rs} - \mathbf{c}_{lc}) - \chi(\mathbf{q} - \mathbf{c}_{lc}), 2\pi).$$

4.2. Simulations. Numerical simulation results are presented to validate the correctness of the proposed method for selecting the shortest generalized Dubins curve.

In Section 3, for the different position relationships between the starting and ending points, we provide the method to determine the shortest curve among RS, LS, RL, and LR, with accompanying theoretical proofs. Now we verify the correctness of the proposed method by numerical simulation.

We specify that each simulation combination consists of a starting point, the direction vector of the starting point, and an ending point. Then we give some simulation combinations that have different position

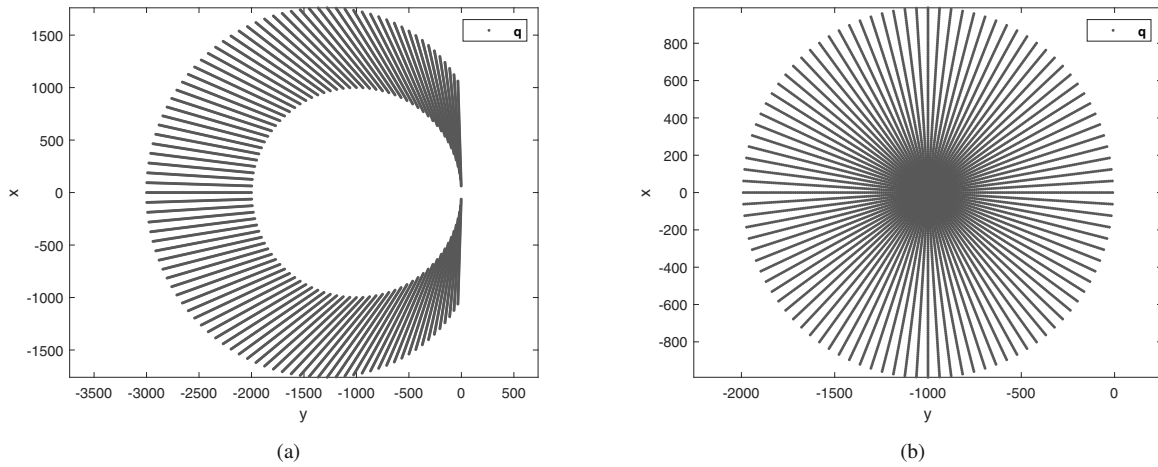


Fig. 6. The positions of the ending point: the ending point is on or outside the turning circles of the starting point and closer to the left-turning circle (a), the ending point is inside the left-turning circle of the starting point (b).

relationships between starting point and ending point. For the simulation combinations where the ending point is on or outside the turning circle of the starting point, we calculate their RS and RL curves, and then present the results to compare the lengths of curves. For the simulation combinations where the ending point is inside the turning circle of the starting point, we calculate their RS and RL curves, or LS and LR curves, and then present the results to compare the lengths of curves.

Certain conditions and parameters utilized in the simulation include the position of starting point denoted as $\mathbf{p} = [0, 0]^T$, the direction vector of starting point denoted as $\mathbf{r}_p = [1, 0]^T$, and the radius of turning circles denoted as $\rho = 1000$.

Example 1. The first simulation is conducted to verify the correctness of proposed shortest generalized Dubins curve selection method in cases where the ending point is on or outside the turning circles of the starting point.

The position and direction of the starting point for the simulation have been previously specified, and now the position of the ending point for the simulation, denoted by \mathbf{q} , is provided. Write $\mathbf{q} = [q_x, q_y]^T$, and let

$$\begin{cases} q_x = (2000 \cdot \sin \frac{n\pi}{100} + 10m) \cdot \cos \frac{n\pi}{100}, \\ q_y = -(2000 \cdot \sin \frac{n\pi}{100} + 10m) \cdot \sin \frac{n\pi}{100}, \end{cases}$$

where $m, n \in \mathbb{Z}$, $0 \leq m \leq 100$, $1 \leq n \leq 99$, which indicates that \mathbf{q} lies on or outside the turning circles of \mathbf{p} and is closer to the left-turning circle. The positions of \mathbf{q} are illustrated in Fig. 6(a).

With the distance calculation method of RS and LS curves presented in Section 4.1, we get the results as

shown in Figs. 7(a) and (b), which show that the LS curve is consistently shorter than the RS curve in this case.

Next, do not change the value of q_x , but let

$$q_y = \left(2000 \cdot \sin \frac{n\pi}{100} + 10m\right) \cdot \sin \frac{n\pi}{100},$$

where $m, n \in \mathbb{Z}$, $0 \leq m \leq 100$, $1 \leq n \leq 99$, which indicates that \mathbf{q} is closer to the right-turning circle.

Similarly, we get the results shown in Figs. 7(c) and 7(d), which show that the RS curve is consistently shorter than the LS curve in this case. ♦

Example 2. In contrast to Example 1, this simulation verifies the correctness of proposed method where the ending point is inside the turning circles of the starting point.

Therefore, we write $\mathbf{q} = [q_x, q_y]^T$, and let

$$q_x = 0, q_y = -1000,$$

or

$$\begin{cases} q_x = 10m \cdot \cos \frac{n\pi}{50}, \\ q_y = -1000 + 10m \cdot \sin \frac{n\pi}{50}, \end{cases}$$

where $m, n \in \mathbb{Z}$, $1 \leq m \leq 99$, $0 \leq n \leq 99$, which indicates that \mathbf{q} lies inside the left-turning circle of \mathbf{p} . The positions of \mathbf{q} are illustrated in Fig. 6(b).

With the distance calculation method of RS and RL curves presented in Section 4.1, we get the results shown in Figs. 8(a) and (b), which show that the RL curve is consistently shorter than the RS curve when \mathbf{q} is inside the left-turning circle of \mathbf{p} .

Then we do not change the value of q_x , but let

$$q_y = 1000,$$

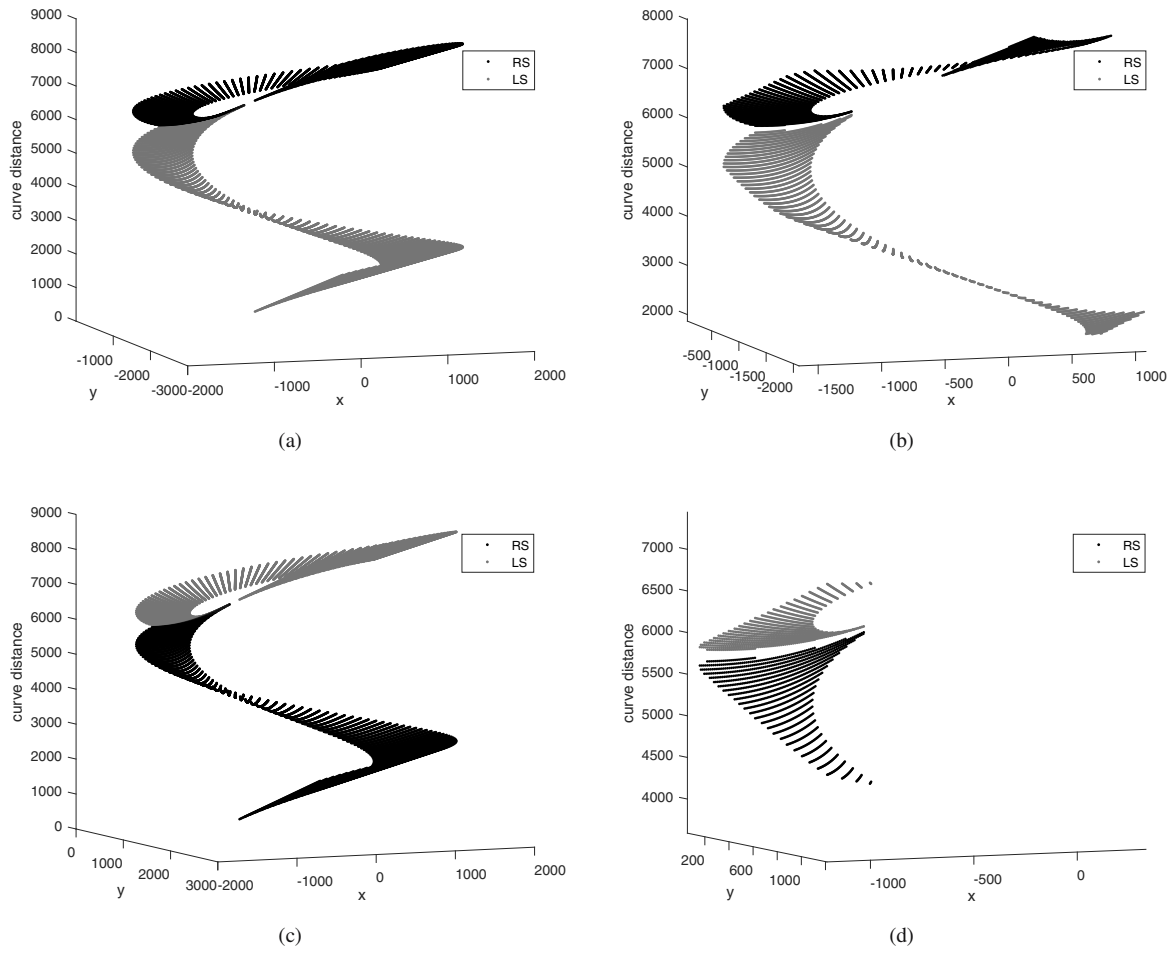


Fig. 7. The distance of the RS and LS curves when the ending point is on or outside the turning circles of the starting point: The distance of the RS and LS curves when the ending point is closer to the left-turning circle (a), the enlargement of (a) (b), the distance of the RS and LS curves when the ending point is closer to the right-turning circle (c), the enlargement of (c) (d).

or

$$q_y = 1000 + 10m \cdot \sin \frac{n\pi}{50},$$

where $m, n \in \mathbb{Z}, 1 \leq m \leq 99, 0 \leq n \leq 99$, which indicates that \mathbf{q} lies inside the right-turning circle of \mathbf{p} .

Similarly, we get the results shown in Figs. 8(c) and (d), which show that the LR curve is consistently shorter than the LS curve when \mathbf{q} is inside the right-turning circle of \mathbf{p} . ♦

5. Conclusions

This paper examines the problem of quickly generating the shortest generalized Dubins path during the forced landing of aircraft. Through theoretical analysis and numerical simulations, the paper determines the shortest path among the four possible generalized Dubins curves RS, LS, RL, and LR based on the relative positions of the forced landing starting and ending points.

Specifically, when the ending point is located on or outside the turning circles of the starting point, the RS curve is identified as the shortest path if the ending point is closer to the right-turning circle, while the LS curve is the shortest when the ending point is closer to the left-turning circle. Moreover, the RL curve is determined to be the shortest when the ending point is situated inside the left-turning circle, and the LR curve is found to be the shortest when the ending point is within the right-turning circle.

According to the aforementioned conclusions, we proceed with a direct computation of the shortest distance from the aircraft's present location to the designated landing site in the event of a forced landing. It eliminates the need to determine the lengths of the four generalized Dubins curves and subsequently compare them to identify the shortest path. This streamlined method simplifies the path generation algorithm for forced landings, facilitating

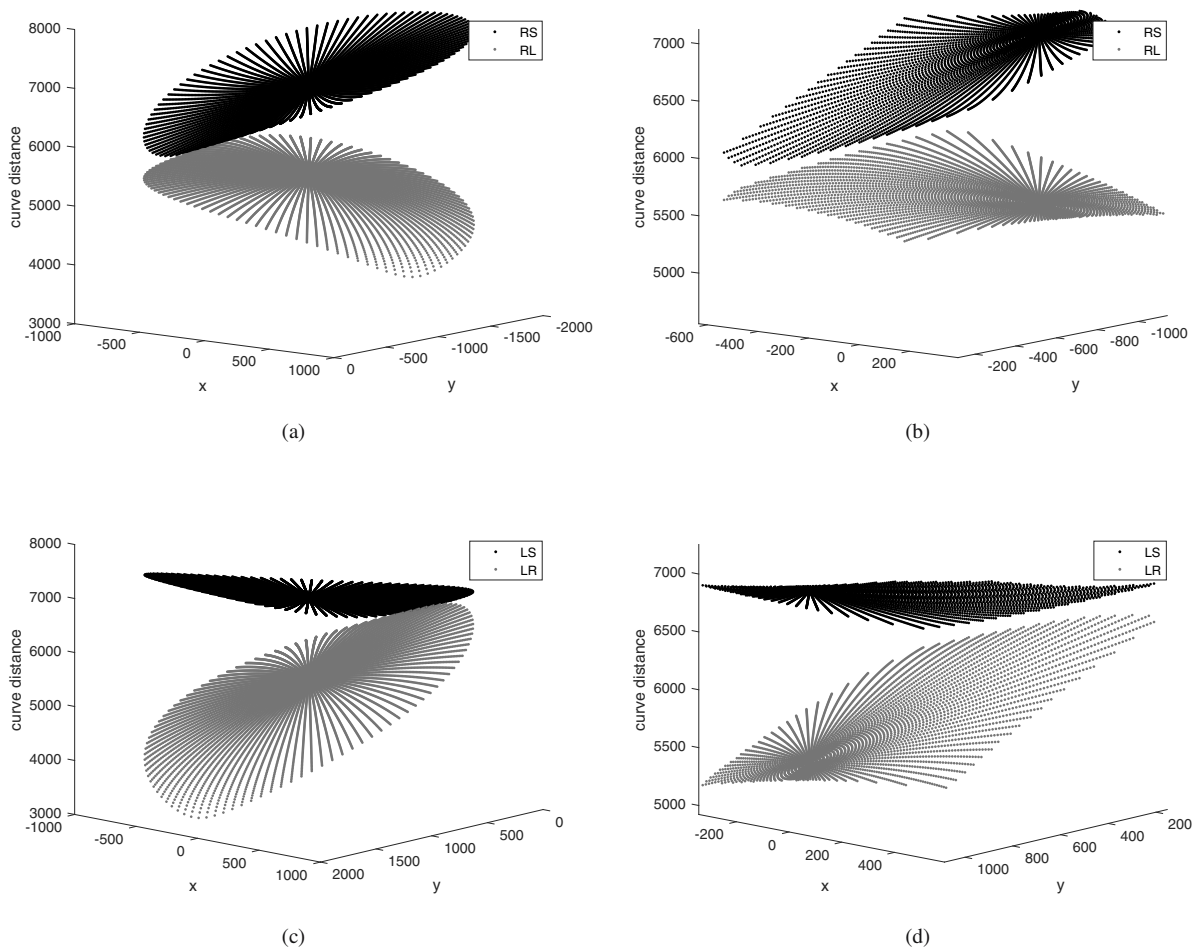


Fig. 8. The distance of the four curves when the ending point is inside the turning circles of the starting point: The distance of the RS and RL curves when the ending point is inside the left-turning circle(a), the enlargement of (a) (b), the distance of the LS and LR curves when the ending point is inside the right-turning circle (c), the enlargement of (c) (d).

real-time distance calculations.

Acknowledgment

This work was supported in part by the National Natural Science Foundation of China under Grant 61973055 and in part by Natural Science Foundation of Sichuan Province of China under Grant 2023NSFSC0511.

References

Chen, Z. (2020). On Dubins paths to a circle, *Automatica* **117**: 108996.
 Chen, Z. and Shima, T. (2019a). Relaxed Dubins problems through three points, *27th Mediterranean Conference on Control and Automation (MED)*, Akko, Israel, pp. 501–506.
 Chen, Z. and Shima, T. (2019b). Shortest Dubins paths through three points, *Automatica* **105**: 368–375.

Drchal, J., Faigl, J. and Váňa, P. (2020). WiSM: Windowing surrogate model for evaluation of curvature-constrained tours with dubins vehicle, *IEEE Transactions on Cybernetics* **52**(2): 1302–1311.
 Dubins, L.E. (1957). On curves of minimal length with a constraint on average curvature, and with prescribed initial and terminal positions and tangents, *American Journal of Mathematics* **79**(3): 497–516.
 Eng, P. (2011). *Path Planning, Guidance and Control for a UAV Forced Landing*, PhD thesis, Queensland University of Technology.
 Gao, X.-Z., Hou, Z.-X., Zhu, X.-F., Zhang, J.-T. and Chen, X.-Q. (2013). The shortest path planning for manoeuvres of UAV, *Acta Polytechnica Hungarica* **10**(1): 221–239.
 Guo, A., Zhou, Z., Wang, R., Zhao, X. and Zhu, X. (2021). Vector field path following of a full-wing solar-powered unmanned aerial vehicle (UAV) landing based on dubins path: a lesson from multiple landing failures, *The Aeronautical Journal* **125**(1290): 1283–1312.

- Gupta Manyam, S., Casbeer, D.W., Von Moll, A. and Fuchs, Z. (2022). Shortest Dubins paths to intercept a target moving on a circle, *Journal of Guidance, Control, and Dynamics* **45**(11): 2107–2120.
- Haghighi, H., Delahaye, D. and Asadi, D. (2022). Performance-based emergency landing trajectory planning applying meta-heuristic and dubins paths, *Applied Soft Computing* **117**: 108453.
- Ismail, A., Tuyishimire, E. and Bagula, A. (2018). Generating dubins path for fixed wing UAVs in search missions, *Ubiquitous Networking: 4th International Symposium, UNet 2018, Hammamet, Tunisia*, Springer, pp. 347–358.
- Izuta, S. and Takahashi, M. (2017). Path planning to improve reachability in a forced landing, *Journal of Intelligent & Robotic Systems* **86**(2): 291–307.
- Kim, Y.-W., Lee, D.-Y., Tahk, M.-J. and Lee, C.-H. (2020). A new path planning algorithm for forced landing of UAVs in emergency using velocity prediction method, *28th Mediterranean Conference on Control and Automation (MED), Saint-Raphael, France*, pp. 62–66.
- Liu, G., Wu, S., Zhu, L., Wang, J. and Lv, Q. (2022). Fast and smooth trajectory planning for a class of linear systems based on parameter and constraint reduction, *International Journal of Applied Mathematics and Computer Science* **32**(1): 11–21.
- Manyam, S.G., Casbeer, D., Von Moll, A. and Fuchs, Z. (2019a). Optimal Dubins paths to intercept a moving target on a circle, *American Control Conference (ACC), Philadelphia, PA, USA*, pp. 828–834.
- Manyam, S.G., Casbeer, D., Von Moll, A.L. and Fuchs, Z. (2019b). Shortest Dubins path to a circle, *AIAA Scitech 2019 Forum*, p. 0919.
- Manyam, S.G. and Rathinam, S. (2018). On tightly bounding the dubins traveling salesman's optimum, *Journal of Dynamic Systems, Measurement, and Control* **140**(7): 071013.
- Parlangeli, G. (2019a). A low-complexity algorithm for shortest dubins paths with intermediate via points, *2019 27th Mediterranean Conference on Control and Automation (MED), Akko, Israel*, pp. 495–500.
- Parlangeli, G. (2019b). Shortest paths for Dubins vehicles in presence of via points, *IFAC-PapersOnLine* **52**(8): 295–300.
- Váňa, P. and Faigl, J. (2022). Bounding optimal headings in the Dubins touring problem, *Proceedings of the 37th ACM/SIGAPP Symposium on Applied Computing, Brno, Czech Republic*, pp. 770–773.
- Váňa, P., Sláma, J., Faigl, J. and Pačes, P. (2018). Any-time trajectory planning for safe emergency landing, *2018 IEEE/RSJ International Conference on Intelligent Robots and Systems (IROS), Madrid, Spain*, pp. 5691–5696.
- Min Tian** received her BS degree in automation from the School of Automation Engineering, University of Electronic Science and Technology of China, in 2024. Now she is studying for her MS degree from the School of Automation Engineering, University of Electronic Science and Technology of China. Her research interests focus on navigation, guidance and control.
- Yingjing Shi** received his PhD degree from the Harbin Institute of Technology, China, in 2008. Currently, he is an associate professor with University of Electronic Science and Technology of China. His research interests include aircraft control, multi-agent systems and computer vision.
- Rui Li** received her PhD degree in control science and engineering from the Harbin Institute of Technology, China, in 2008. She is currently a professor at the University of Electronic Science and Technology of China. Her research interests include multi-agent systems, optimal control, computer vision and aircraft control.
- Esteban Tlelo Cuautle** received his PhD degree from Instituto Nacional de Astrofísica, Óptica y Electrónica (INAOE), Mexico in 2000. He is currently a professor at INAOE. He is a member in the National System for Researchers (SNI-CONACyT-México) and an IEEE Senior Member. His research interests include multi-objective optimization, principle of automatic control, UAV control, robot kinematics and design and applications of chaotic CASS.

Received: 28 June 2024

Revised: 28 October 2024

Accepted: 10 February 2025